MULTI-WAVELENGTH OBSERVATIONS OF MAGELLANIC SNRs

M. D. Filipović[1], J. L. Payne[2], F. Haberl[3], W. Pietsch[3], P. F. Winkler[4], E. J. Crawford[1], A. Y. Horta[1] and F. H. Stootman[1]

[1]University of Western Sydney, Locked Bag 1797, Penrith South, DC, NSW 1797, Australia
[2]Centre for Astronomy, James Cook University, Townsville, Australia
[3]Max-Planck-Institut für extraterrestrische Physik, Giessenbachstrasse, D-85741, Garching, Germany
[4]Department of Physics, Middlebury College, Middlebury, VT 05753, USA

ABSTRACT

The study of supernova remnants (SNRs) and their elemental enrichment of the interstellar medium (ISM) at different wavelength domains including radio, optical and X-ray, allow for a better understanding of these remnants and their environments. The Small (SMC) and Large Magellanic Clouds (LMC) offer an ideal laboratory, since they are near enough to be resolved, yet located at relatively known distances. Here we present preliminary results of three separate studies involving SNRs in the optical, radio and X-ray domain. First, we report recent *XMM-Newton* observations of three (3) known (DEM S5, SNR B0050-72.8 and SNR B0058-71.8) and one candidate (HFPK 334) remnant in the SMC. Next, is the possible discovery of 16 new optical SNRs and super-bubbles in the SMC; this may well double the population of known remnants in that galaxy. Finally, we present results from new high resolution Australia Telescope Compact Array (ATCA) observations of LMC SNR J0519-6926.

INTRODUCTION

The physics that underlie interactions between supernova remnants (SNRs) and the surrounding interstellar medium (ISM) is best studied through the use of multi-wavelength astronomy. However, many Galactic SNRs have distance uncertainties of at least a factor of 2 (Seward 2006). Alves (2004) reviewed distance and structure studies of the Large Magellanic Cloud (LMC), finding that the average of 14 recent measurements converge to a modulus of 18.50 ± 0.02 magnitude ($D \sim 50.1$ kpc). These results demonstrate a high level of consistency and the possibility that a consensus on the LMC distance has been reached. Using eclipsing binaries, Hilditch (2005) estimated a distance modulus of 18.91 ± 0.03 ($D \sim 60.6$ kpc) for the SMC, representing one of the most precise distance determinations to that galaxy. This degree of certainty allows the use of Magellanic Cloud (MC) astronomical objects, including SNRs, to determine their properties as well as that of their surrounding ISM. Today a total number of eighteen classified SNRs are known in the SMC (see Table 1). Related articles describing these include Filipović et al. (2002, 2005), Payne et al. (2007), van der Heyden et al. (2004), Dickel et al. (2001), Mathewson et al. (1984), Mills et al. (1982), Hughes & Smith (1994), Nazé et al. (2004) and references therein.

TABLE 1: SNRs and SNR candidates in the SMC. The radio spectral index (α) is taken from Filipović et al. (2005) and [S II]/Hα ratio from Payne et al. (2007).

No	SNR Name	R.A. (J2000)	Dec (J2000)	D [pc]	$S_{1\,GHz}$ [Jy]	α	[S II]/Hα	Other Names
1	DEM S5	00 41 00.1	−73 36 30.0	68.4×62.6	0.057	−0.9	0.8	HFPK 530
2	DEM S32	00 46 37.6	−73 07 56.6	40.7×46.5	0.036	−0.6	0.4	Part of N S19, WW 15
3	J0047-7306	00 47 28.6	−73 06 15.5	32.0×8.7	0.035	−0.1	1.2	part of N S19
4	HFPK 419	00 47 36.5	−73 09 14.0	44.2×33.7	0.215	−0.6	0.4	part of N S19, HFPK 419
5	IKT 2	00 47 16.6	−73 08 43.5	29.1×32	0.500	−0.6	0.4	N S19, DEM S32, WW 16, HFPK 413
6	IKT 4	00 48 20.6	−73 19 39.6	45.1×34.9	0.176	−1.0	0.4	N S24, WW 21, DEM S42, HFPK 454
7	IKT 5	00 49 07.7	−73 14 35.0	48.3	0.034	−0.6	0.7	DEM S49, WW 22, HFPK 437
8	IKT 6	00 51 06.7	−73 21 21.4	42.2	0.137	−0.7	0.5	1E0049.4-7339, WW 24, HFPK 461
9	B0050-72.8	00 52 36.9	−72 37 18.5	42	0.273	−1.0	0.4	N S50, DEM S68, WW 30, HFPK 285
10	N S66D	00 58 00.0	−72 11 01.4	58.2	0.057	0.0	0.4	
11	IKT 16	00 58 17.8	−72 18 07.4	58	0.091	−0.7	0.5	WW 42
12	IKT 18	00 59 27.7	−72 10 09.8	40.7	0.501	−0.8	1.7	N S66, NGC 346, WW 44, HFPK 148
13	B0058-71.8	01 00 23.9	−71 33 41.1	61	0.241	−0.8	[O III]	DEM S108, HFPK 45
14	IKT 21	01 03 17.0	−72 09 45.0	20.9	0.123	−0.5	0.5	N S76C, WW 50
15	1E0102-723	01 04 01.2	−72 01 52.3	5.8×10.5	0.363	−0.6	[O III]	N S76, IKT 22, WW 51, HFPK 107
16	IKT 23	01 05 04.2	−72 23 10.5	55.9	0.112	−0.7	[O III]	DEM S125, WW 52, HFPK 217
17	DEM S128	01 05 24.7	−72 09 20.4	37.8	0.060	−0.5	0.6	IKT 24, WW 53, HFPK 145
18	IKT 25	01 06 27.5	−72 05 34.5	32×23	0.014	−0.7	0.4	DEM S131, WW 54, HFPK 125
19	HFPK 334	01 03 29.5	−72 47 23.2	17.5	0.025	−0.5	—	HFPK334
20	B0113-729	01 13 33.8	−73 17 04.4	21.8	0.108	−0.6	0.4?	N S83C, DEM S147, HFPK 448

OBSERVATIONS

In order to investigate the X-ray source population of the SMC, Haberl & Pietsch (2007) started a systematic analysis of the available *XMM-Newton* data (Jansen et al. 2001). This included their own proprietary data together with data from the public archive. Only observations performed with the EPIC-PN instrument (Struüder et al. 2001) in *Large Window* (LW), *Full Frame* (FF) or *extended Full Frame* (eFF) imaging CCD readout mode were considered. The data were analyzed using the analysis package XMMSAS version 7.0.0.

In the optical domain, there has been much excitement about recent high resolution MC observations. This includes the Magellanic Cloud Emission Line Survey (MCELS), created using the 0.6-m University of Michigan/CTIO Curtis Schmidt telescope, equipped with a SITE 2048 × 2048 CCD. This configuration gave a field of 1.35° at a scale of 2.4″ pixel^{-1}. The detail for SNRs and super-bubbles is stunning.

Both the LMC and SMC were mapped in narrow bands corresponding to Hα, [O III] (5007Å) and [S II] (6716, 6731Å). Matched red and green continuum bands are used to subtract most stars, leaving a generous faint diffuse emission. A 4.5° × 3.5° region, most of the SMC, was covered in 69 overlapping fields, offset such that every point was included in at least four different fields. All data have been flux-calibrated and assembled into mosaic images. For more details see http://www.ctio.noao.edu/mcels/ .

We also present observations of LMC SNR J0519-6926 using the ATCA with a 375-meter baseline at wavelengths of 6 and 3 cm ($\nu \sim 4790$ and 8640 MHz). These observations were performed in 'snap shot' mode, totaling ∼1 hour of integration over a 12 hour period. Source 1934-638 was used for primary calibration and 0530-727 for secondary calibration. More information about the observing procedure (and another source observed during this session, LMC SNR B0513-69) can be found in Bojičić et al. (2007).

RESULTS

In Fig. 1, we show results from our *XMM-Newton* observations of three SNRs not previously studied in detail due to their faintness: DEM S5 (HFPK 530), SNR B0050−72.8 (DEM S68; HFPK 285) and SNR B0058−71.8 (DEM S108; HFPK 45). All three were detected in *ROSAT* PSPC data (Haberl et al. 2000, with catalogue entries given by their HFPK number) and were not yet observed by *XMM-Newton* at the time of the work of van der Heyden et al (2004). They have optical and radio counterparts, but a variety of morphologic features are relatively uncorrelated in different domains, perhaps due to a diversity of local conditions. Another *ROSAT* PSPC source, HFPK 334, (with evidence for spatial extent in the *ROSAT* data and a possible radio counterpart) shows X-ray colours typical for SNRs and we suggest it as a new candidate SNR. Shown also in Fig. 1, it is not seen in the optical.

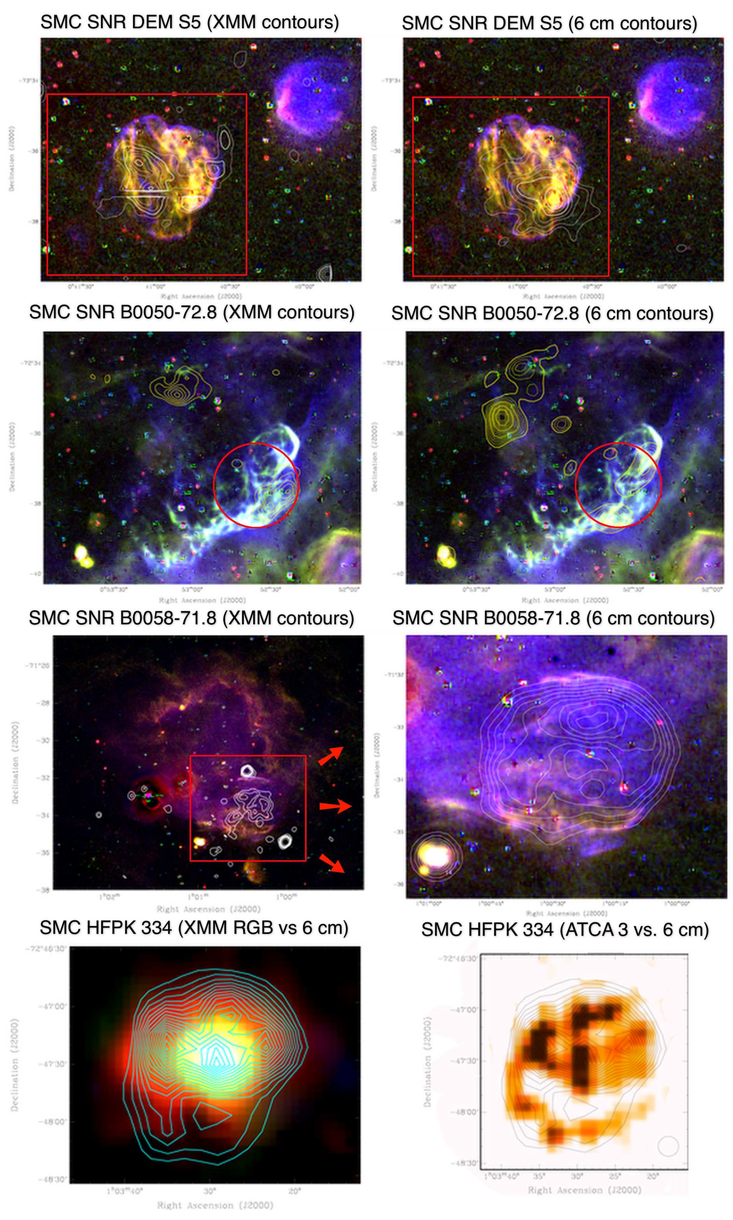

FIGURE 1: Composite MCELS optical images of SNRs DEM S5, B0050-72.8 and B0058-71.8 (RGB represents Hα, [S II] and [O III], respectively, all continuum-subtracted) overlayed with *XMM-Newton* broad-band (left) and ATCA 6 cm contours (right). Extent and position of SNRs are encased in red boxes or circles. Also shown is a composite *XMM-Newton* image of SNR candidate HFPK 334 overlayed with ATCA 6 cm contours (bottom left). Here, RGB represent soft (0.2-1.0 keV), medium (1.0-2.0 keV) and hard (2.0-4.5 keV) X-rays, respectively. A 3 cm ATCA image of HFPK 334 with 6 cm contours is also shown (bottom right). The circle represents the 3 cm resolution of 12″ × 11″.

Further examination of MCELS images as exampled in Fig. 2, have also revealed a total of 16 new optical SNR / super-bubble candidates based on their position, size and morphology. These objects have generous emission in Hα, [O III] and [S II]. They range in diameter from 9 to ∼ 160 pc, suggesting that five are SNR-bubble candidates and two are super-bubbles, the latter based on size greater than 100 pc. This sample is selected by optical observations only, as they are too faint in radio or X-ray to be detected.

Reduction and analysis of our LMC SNR J0519-6926 ATCA image using MIRIAD (Sault & Killeen 2006) and KARMA (Gooch 2006) software packages was performed with exclusion of baselines from the 6th ATCA antenna; the other five antennas were arranged in a compact configuration.

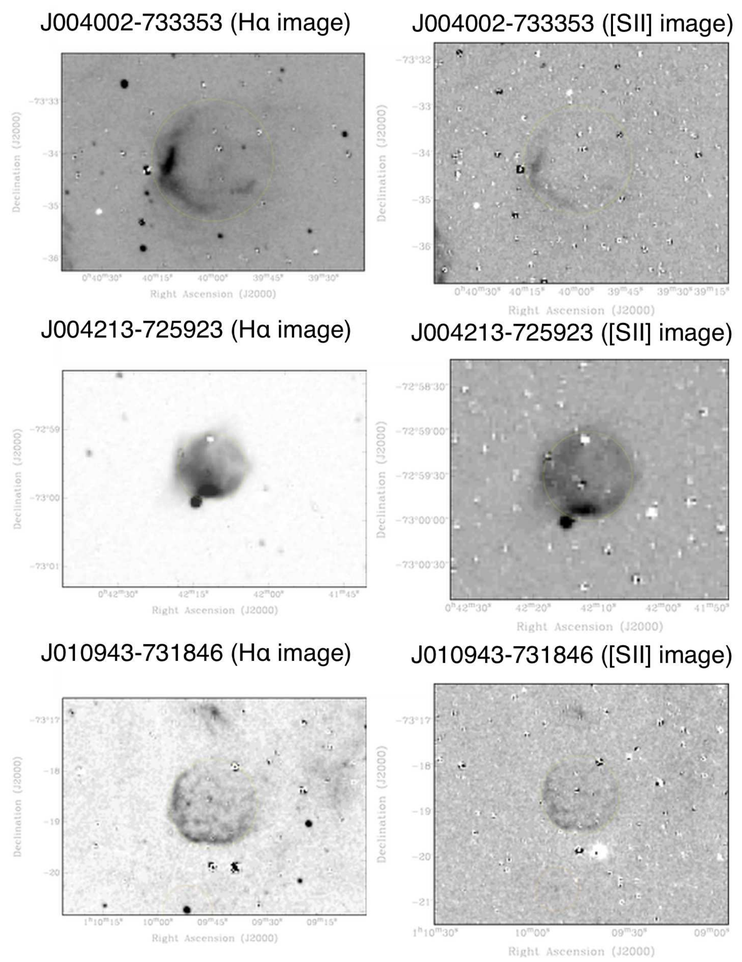

FIGURE 2: Three of 16 optical SNR / super-bubble candidates found in MCELS images based on morphology and significant [S II] and [O III] emission. Comparison of Hα and [S II] images are shown.

A 6 cm image was created having a resolution of 32″ and a 3 cm image with a resolution of 20″; for both, the estimated r.m.s. noise is ∼ 0.4 mJy/beam. Another 3 cm image with a resolution of 32″ was created to compliment the 6 cm image. We also created a spectral index image using MIRIAD in order to further correlate morphology with areas of thermal and non-thermal emission as shown in Fig. 3.

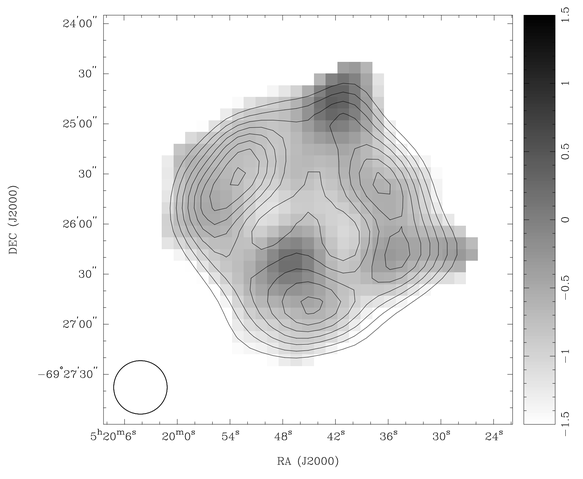

FIGURE 3: Spectral index map (shown as intensity) of SNR J0519-6926 overlaid with 3 cm contours. The black circle in the lower left corner represents the primary beam of 32″.

For LMC SNR J0519-6926, we find a overall spectral index of -0.55 ± 0.07. It has a diameter of 28 ± 1 pc, with no significant polarization (< 1%) and a typical SNR morphology.

At the relatively known distances of the MCs, these identifications and measurements of SNRs lead us to a deeper understanding of these objects and their local ISM environments. We hope to use them in the future to better understand Galactic remnants.

REFERENCES

Alves, D. R., 2004, New Astronomy Reviews, 48, 659
Bojičić, I. S., Filipović, M. D., Parker, Q. A., et al., 2007, MNRAS, 378, 1237
Dickel, J. R., Williams, R. M., Carter, L. M., et al., 2001, AJ, 122, 849
Filipović, M. D., Bohlsen, T., Reid, W., et al., 2002, MNRAS, 335, 1085
Filipović, M. D., Payne, J. L., Reid, W., et al., 2005, MNRAS, 364, 217
Gooch, R., 2006, Karma Users Manual, ATNF
Haberl, F., Filipović, M. D., Pietsch, W., et al., 2000, A&AS, 142, 41
Haberl, F., Pietsch, W., 2007, ArXiv e-prints, 712
Hilditch, R. W., Howarth, I. D., Harries, T. J. 2005, MNRAS, 357, 304
Hughes, J. P., Smith, R. C., 1994, AJ, 107, 1363
Jansen, F., Lumb, D., Altieri, B., et al., 2001, A&A, 365,1
Mathewson, D. S., Ford, V. L., Dopita, M. A., et al., 1984, ApJS, 55,189
Mills, B. Y., Little, A. G., Durdin, J. M., et al., 1982, MNRAS, 200, 1007
Nazé, Y., Manfroid, J., Stevens, I. R., et al., 2004, ApJ, 608, 208
Payne, J. L., White, G. L., Filipović, M. D., et al., 2007, MNRAS, 376, 1793
Sault, R., Killeen, N., 2006, Miriad Users Guide, ATNF
Seward, F. D., Williams, R. M., Chu, Y. -H., et al., 2006, ApJ, 640, 327
Struüder, L., Briel, U., Dennerl, K., et al., 2001, A&A, 365, 18
van der Heyden, K. J., Bleeker, J. A. M., Kaastra, J. S., 2004, A&A, 421, 4031